

# Catalytic Oxidation of Toluene over Y-Ba-Cu Perovskites: Activity and X-Ray Photoelectron Spectroscopy Studies

S. Lars T. Andersson

Department of Chemical Technology, Chemical Center, University of Lund, P.O. Box 124, S-221 00 Lund, Sweden

The catalytic oxidation of toluene over Y-Ba-Cu-O phases has been studied. At low oxygen pressures, low rates and a certain selectivity for benzaldehyde occurs, whereas at high oxygen pressures, high rates with complete selectivity for carbon oxides is obtained. X-Ray photoelectron spectroscopy (XPS) analysis of used catalysts identifies the presence of predominantly Cu<sup>I</sup> states when used at conditions showing some selectivity, whereas after use under combustion conditions, Cu<sup>II</sup> states are found. The initial activities of freshly charged catalysts with different oxygen contents are different, but are greatly affected by pre-reduction/oxidation treatments, which yield similar activities. Large variations in surface Y-Ba-Cu concentrations with various treatments are observed. In particular, high surface copper concentrations may be obtained after extensive reduction-oxidation cycles. The catalyst is modelled as highly dispersed copper oxide over a support with variable oxygen content. The different behaviour of the reduced and oxidized catalysts can be interpreted by bond valence calculations, suggesting that the selectivity over reduced forms is connected to more nucleophilic oxygen species and that the cations are milder oxidants than for the oxidized forms. The inferior selectivity compared with the ammoxidation of toluene, but comparable activity, suggests the formation of a reactive benzylic intermediate in the first step for both reactions.

The YBa<sub>2</sub>Cu<sub>3</sub>O<sub>6+x</sub> compound has recently found various applications in catalysis. Its catalytic properties have been investigated for reactions such as NO + CO,<sup>1</sup> oxidation of CO<sup>2,3</sup> and CH<sub>4</sub>,<sup>4</sup> oxidation and dehydrogenation of methanol<sup>5-7</sup> and ammoxidation of toluene.<sup>8-12</sup> At low oxygen pressures this material is equally as active and selective for the ammoxidation of toluene as vanadium oxide catalysts, whereas at high oxygen pressure, total combustion is predominant.<sup>9</sup> In the search for materials selective in the oxidation of toluene, it was therefore of great interest to investigate the properties of this material. Also a comparison with the properties for ammoxidation of toluene could reveal mechanistic features of both reactions. It is, however, not excluded that in ammoxidation the chemical state of the surface is different from that during oxidation of hydrocarbons.

The catalytic performance of YBa<sub>2</sub>Cu<sub>3</sub>O<sub>6+x</sub> is strongly dependent on the oxygen pressure, which was correlated to the predominant occurrence of Cu<sup>I</sup> states at low and Cu<sup>II</sup> states at high pressures, as verified by XPS measurements.<sup>10,11</sup> The formation almost exclusively of Cu<sup>I</sup> states is not compatible with the bulk structure of YBa<sub>2</sub>Cu<sub>3</sub>O<sub>6+x</sub> retained at the surface. It is also known that the surfaces of these materials degrade to various products when exposed to H<sub>2</sub>O and CO<sub>2</sub>.<sup>13,14</sup> Substitution of Zn for Cu at various levels produces catalytic effects that are best explained by a contribution from both bulk and surface compounds.<sup>11</sup> The possible interactions are not well known and these materials need to be characterized further.

## Experimental

The tetragonal YBa<sub>2</sub>Cu<sub>3</sub>O<sub>6+x</sub> and orthorhombic YBa<sub>2</sub>Cu<sub>3</sub>O<sub>7-x</sub> catalysts were from the same batches as prepared by the ceramic route in earlier studies,<sup>10,11</sup> where detailed descriptions are given. For simplicity the notations YBa<sub>2</sub>Cu<sub>3</sub>O<sub>6</sub> and YBa<sub>2</sub>Cu<sub>3</sub>O<sub>7</sub> will be used.

XPS measurements were performed on a Kratos

XSAM800 instrument. An Al anode (1486.6 eV†) was used. The slit width was set at 40° and the analyser was operated at 40 eV pass energy and high magnification. Charging effects were corrected for by adjusting the main C 1s peak to a position at 285.0 eV. Analysis of the spectra was performed with the DS800 data system. Sensitivity factors used in the quantitative analysis were 1.0 for O 1s, 1.15 for Y 3d, 1.54 for Ba 4d and 2.65 for Cu 2p<sub>3/2</sub> as in earlier studies.<sup>10,11</sup> Samples initially containing mainly Cu<sup>I</sup> showed similar Cu spectra after a long time of exposure to air (6 months) to those when transferred under nitrogen directly from reactor to spectrometer.

The catalytic activity for oxidation of toluene was measured in a conventional microreactor flow apparatus at atmospheric pressure. The total flow rate was 18-36 dm<sup>3</sup> h<sup>-1</sup> with a feed composition of 9.8 Torr‡ toluene, while the oxygen pressure was varied from 0 to 200 Torr with a balance of nitrogen. The reaction temperature was kept constant at 340 °C. The catalyst bed contained 0.15-0.4 g catalyst diluted with inert quartz. The on-line gas chromatographic (GC) analytical methods have been described in detail elsewhere.<sup>15</sup> The reactor was operated in the differential mode with conversions below 15%, and was operated for at least 1 h at each condition.

## Results

### Activity Measurements over YBa<sub>2</sub>Cu<sub>3</sub>O<sub>6</sub>

The catalytic measurements were carried out after an initial treatment in nitrogen flow at 400 °C for 1 h. Thereafter, the appropriate toluene, oxygen and nitrogen mixtures were passed over the catalyst bed with the oxygen partial pressure varied from low to high initially, and thereafter from high to low. At each condition data were accumulated for ca. 1 h when steady state was almost attained. The only products

† 1 eV ≈ 1.602 × 10<sup>-19</sup> J.

‡ 1 Torr = 101 325/760 Pa.

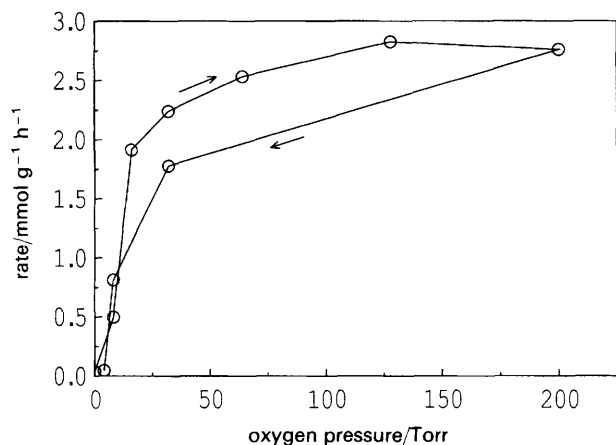


**Fig. 1** Rate of oxidation of toluene at 340°C over  $\text{YBa}_2\text{Cu}_3\text{O}_6$ , *in situ* pretreated in nitrogen at 400°C for 1 h, as a function of oxygen partial pressure. Arrows indicate the direction in which the oxygen pressure was varied, starting from 0 Torr. (Catalyst analysed by XPS after completed cycle, see Table 1)

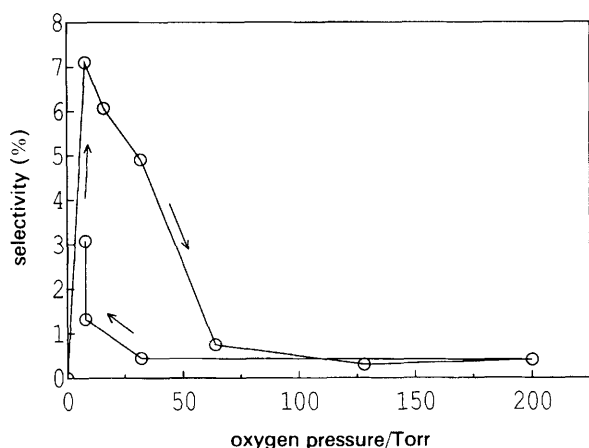


**Fig. 2** Selectivity for benzaldehyde in oxidation of toluene at 340°C over  $\text{YBa}_2\text{Cu}_3\text{O}_6$ , *in situ* pretreated in nitrogen at 400°C for 1 h, as a function of oxygen partial pressure. Comments as in Fig. 1

detected are benzaldehyde and carbon oxides. The results are presented in Fig. 1 and 2, showing the rate of oxidation of toluene and selectivity for benzaldehyde as functions of oxygen pressure. With increased oxygen partial pressure, between 10 and 50 Torr, the rate is greatly increased to the high level maintained at the highest oxygen partial pressures. When returning from high oxygen partial pressure back to low pressures, the original curve is not quite followed. Selectivity for benzaldehyde shows initially a maximum at low oxygen pressures, and a hysteresis effect is observed when returning from high oxygen partial pressure.

#### Activity Measurements over $\text{YBa}_2\text{Cu}_3\text{O}_7$

Catalytic measurements were carried out over both the oxidized and the reduced form of this material. Fig. 3 and 4 show the oxygen pressure dependences of the rate of toluene oxidation and benzaldehyde selectivity, respectively, over  $\text{YBa}_2\text{Cu}_3\text{O}_7$  pretreated in oxygen at 400°C for 1 h. The initial experiment was carried out at 200 Torr oxygen, and with decreased oxygen partial pressure the rate was constant down to ca. 50 Torr oxygen, but decreased at lower pressures. At 0 Torr of oxygen, conversion is still observed.

Thereafter, on increasing the pressure, considerably higher activity than earlier is observed. When the oxygen pressure is returned to 200 Torr, the activity has almost tripled, but is not quite as high as that for  $\text{YBa}_2\text{Cu}_3\text{O}_6$ , cf. Fig. 1. The selectivity, see Fig. 4, shows a similar behaviour to  $\text{YBa}_2\text{Cu}_3\text{O}_6$  (Fig. 2) when going from 0 to high oxygen partial pressure, with a minimum at low pressures. The final selectivity at 200 Torr of oxygen is considerably lower than that measured initially at the start of the whole experiment.

The reduced form of  $\text{YBa}_2\text{Cu}_3\text{O}_7$  was obtained by pretreatment in nitrogen at 400°C for 1 h. The reaction rate was thereafter followed as a function of time-on-stream at an oxygen partial pressure of 12 Torr. As seen in Fig. 5(a), the rate increases with time-on-stream and the steady state is almost obtained after ca. 45–60 min. The selectivity, see Fig. 6(a), also increases to a steady-state value after ca. 45–60 min. After this experiment the catalyst was further reduced by continued treatment without oxygen and also additionally without toluene, and then experiments with 10 Torr of oxygen were performed. The rate, see Fig. 5(b), increases during the first 45 min to an almost constant value thereafter. The rate is, however, considerably higher than before the extensive reductive treatment. The selectivity shows a similar behaviour except for an initially decreasing value [Fig. 6(b)].

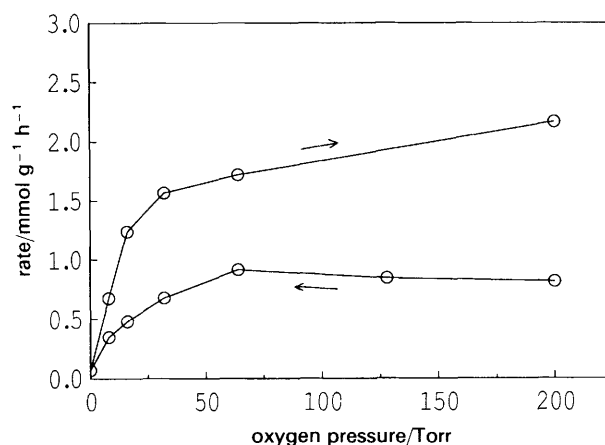


**Fig. 3** Rate of oxidation of toluene at 340°C over  $\text{YBa}_2\text{Cu}_3\text{O}_7$ , *in situ* pretreated in oxygen at 400°C for 1 h, as a function of oxygen partial pressure. Arrows indicate the direction in which oxygen pressure was varied, starting from 200 Torr. (Catalyst analysed by XPS after completed cycle, see Table 1)

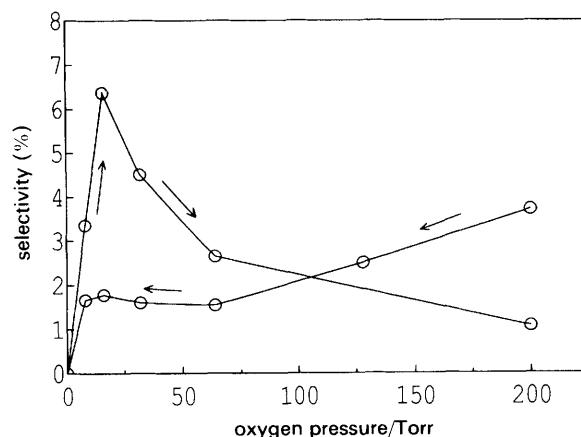


**Fig. 4** Selectivity for benzaldehyde in oxidation of toluene at 340°C over  $\text{YBa}_2\text{Cu}_3\text{O}_7$ , *in situ* pretreated in oxygen at 400°C for 1 h, as a function of oxygen partial pressure. Comments as in Fig. 3

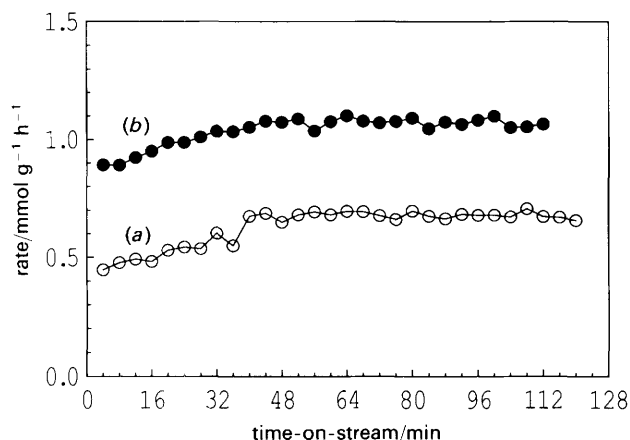


**Fig. 5** Rate of oxidation of toluene at 340 °C over  $\text{YBa}_2\text{Cu}_3\text{O}_7$ , as a function of time-on-stream; extensively used catalyst, pretreated in nitrogen at 400 °C for 1 h. Initial experiment (a)  $P_{\text{O}_2} = 12$  Torr. Thereafter, extensive use at  $P_{\text{O}_2} = 0$  Torr and/or  $P_{\text{toluene}} = 0$  Torr before last experiment. (b)  $P_{\text{O}_2} = 10$  Torr. [Catalyst analysed by XPS after experiment (b)]

The evolution of activity with reductive treatment and use at low oxygen partial pressures was further investigated for a  $\text{YBa}_2\text{Cu}_3\text{O}_7$  sample after pretreatment in nitrogen at 450 °C for 1 h. Fig. 7 shows the resulting rate of toluene oxidation as a function of oxygen partial pressure. The rate at 12 Torr oxygen has increased five-fold after the reductive treatment at 0 Torr of oxygen, compared with the initial measurement. However, the measurements at various oxygen pressures below 50 Torr produce remarkably reproducible data with an almost linear oxygen pressure dependence of the reaction rate. The selectivity is also improved by reduction at 0 Torr of oxygen and shows again an optimum at low oxygen pressures. However, after the discontinued experiment, treatment with 200 Torr of oxygen followed by 15 h at room temperature, marked by an asterisk, a considerably increased selectivity at continued use at 14 Torr of oxygen was observed. Thereafter, the selectivity decreases at increased oxygen pressures. These data clearly indicate the importance of the pretreatment of the samples for the evolution of the active surfaces.

### Characterization by XPS

#### Surface Degradation

The  $\text{YBa}_2\text{Cu}_3\text{O}_6$  and  $\text{YBa}_2\text{Cu}_3\text{O}_7$  catalysts were investigated by XPS after the various completed activity measurements,

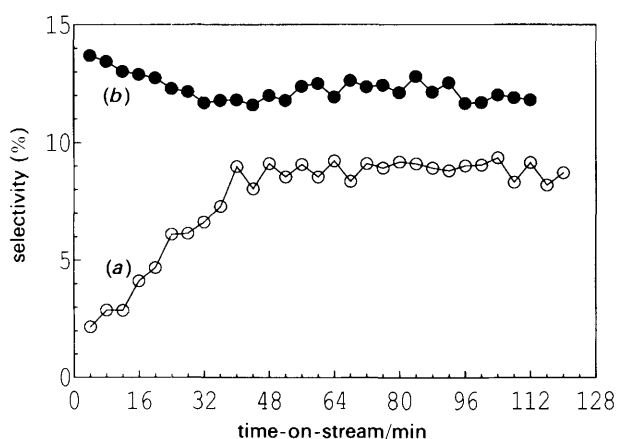


**Fig. 6** Selectivity for benzaldehyde in oxidation of toluene at 340 °C over  $\text{YBa}_2\text{Cu}_3\text{O}_7$ , as a function of time-on-stream. Conditions and notations as in Fig. 5

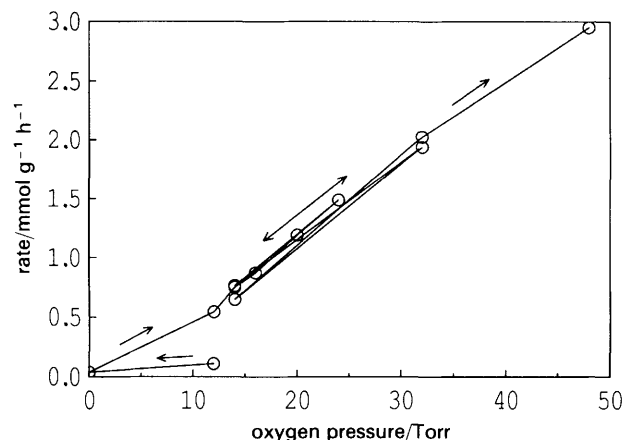


**Fig. 7** Rate of oxidation of toluene at 340 °C over  $\text{YBa}_2\text{Cu}_3\text{O}_7$ , *in situ* pretreated in nitrogen at 450 °C for 1 h, as a function of oxygen partial pressure. Arrows indicate the direction in which oxygen pressure was varied. (Catalyst analysed by XPS after completed experiment)

presented in Fig. 1–8. Table 1 shows binding energies ( $E_b$ ) and half-widths for the various core levels measured, and spectra for O 1s, Ba 3d, Cu  $L_{3,4,5}$  and the valence band are presented in Fig. 9–12, respectively. The major differences are observed in the Cu 2p lines when comparing differently used catalysts, whereas for the Y and Ba lines minor differences are observed, mainly when comparing fresh and used samples.

Note that all lines for fresh samples show contributions from two components, one major contribution at higher  $E_b$  and one minor one at lower  $E_b$ . The former is due to surface degradation products, signified by peaks of O 1s at *ca.* 531.5 eV, Y  $3d_{5/2}$  at 157.5 eV, Ba  $3d_{5/2}$  at 779.9 eV and Cu  $2p_{3/2}$  at *ca.* 934.4 eV with a strong satellite at *ca.* 942.5 eV, as shown elsewhere.<sup>13</sup> These products may constitute  $\text{Ba}(\text{OH})_2$ ,  $\text{BaCO}_3$ ,  $\text{Y}_2\text{BaCuO}_5$ ,  $\text{CuO}$ ,  $\text{BaCuO}_2$ ,  $\text{Ba}_2\text{Cu}(\text{OH})_6$ ,  $\text{Y}_2\text{O}_3$  and  $\text{Y}(\text{OH})_3$ .<sup>16–22</sup> The carbonate compounds are evident, considering the strong C 1s line for  $\text{CO}_3^{2-}$  species for all samples (at *ca.* 289.5 eV). Furthermore, for all fresh samples a clear contribution from the bulk compounds,  $\text{YBa}_2\text{Cu}_3\text{O}_6$  and  $\text{YBa}_2\text{Cu}_3\text{O}_7$ , of *ca.* 10–30% in all spectra is seen. Therefore, the surface layer thickness may be estimated to be the length of *ca.* one electron mean free path, equivalent to *ca.*

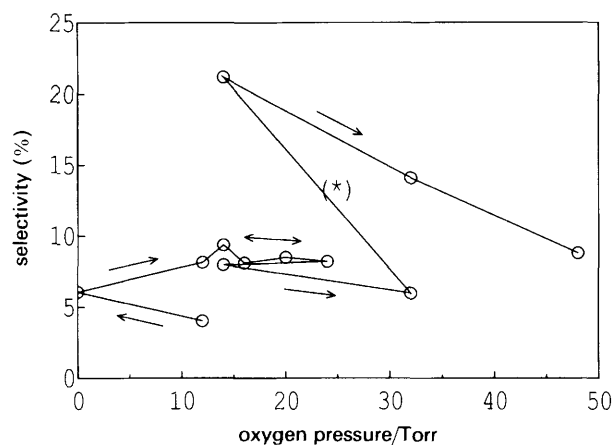


**Fig. 8** Selectivity for benzaldehyde in oxidation of toluene at 340 °C over  $\text{YBa}_2\text{Cu}_3\text{O}_7$ , *in situ* pretreated in nitrogen at 450 °C for 1 h, as a function of oxygen partial pressure. Comments as in Fig. 7. (Between points marked \*, the catalyst was treated in 200 Torr of oxygen, after which it was kept for 15 h at room temperature)

**Table 1** Core line binding energies<sup>a</sup> (eV) and half widths<sup>b</sup> (eV) for Y–Ba–Cu–O catalysts, as received and used at different conditions

sample	O 1s	Ba 3d <sub>5/2</sub>	Ba 4d	Cu 2p <sub>3/2</sub>		<i>I</i> <sub>sat</sub> / <i>I</i> <sub>main</sub>	Cu LMM <sup>c</sup>	Auger param.
				sat	main			
YBaCuO <sub>7</sub>								
fresh	531.4 <sup>d</sup> (2.3)	779.8 (2.3)	89.2 (4.3)	942.3–933.9 (5.0)	933.9 (2.9)	0.57	917.5	1851.0
used (200 Torr O <sub>2</sub> )	531.6 <sup>d</sup> (2.2)	779.9 (2.1)	89.4 (2.0)	942.2–933.5 (4.4)	933.5 (2.8)	0.48	918.2	1851.7
used (48 Torr O <sub>2</sub> )	531.5 <sup>d</sup> (2.3)	779.9 (2.3)	89.3 (2.3)	942.2–933.5 (4.8)	933.5 (2.8)	0.53	918.1	1851.6
used (10 Torr O <sub>2</sub> )	531.5 <sup>d</sup> (3.4)	779.9 (2.3)	89.4 (4.4)	—	932.7 (1.7)	0	916.5	1849.2
YBaCuO <sub>6</sub>								
used (4–8 Torr O <sub>2</sub> )	531.5 (2.3)	779.9 (2.1)	89.3 (2.2)	—	932.7 (1.7)	0	916.5	1849.2
surface <sup>e</sup>	531.5–530.8	779.9	89.4	942.5–934.4				
bulk <sup>e</sup>	528.8	778.6	88.3	942.5–934–932.6				
CuO	530.0 (1.7)			942.1–934.0 (3.4)		0.65	917.7	1851.7
Cu <sub>2</sub> O	530.9 (1.6)			—	932.9 (1.6)	0	916.4	1849.3
Cu	—			—	932.6	0	918.6	1851.2

<sup>a</sup> Referenced to C 1s = 285.0 eV. Used samples referenced to Ba 3d<sub>5/2</sub> = 779.9 eV. Positions at peak maxima. <sup>b</sup> Given within brackets.

<sup>c</sup> L<sub>3</sub>M<sub>4,5</sub>M<sub>4,5</sub> kinetic energy. <sup>d</sup> Two components. <sup>e</sup> See ref. 13.

15–25 Å, since the intensity depends on the depth as  $\exp(-\lambda/d)$ . Upon use of the samples in oxidation of toluene at various oxygen pressures, the surface layer thickness increases, since no trace of the bulk compounds is visible in the various spectra. This is most clearly seen in the Ba 3d spectra presented in Fig. 10. The O 1s spectra in Fig. 9 show the development of other features at higher  $E_b$  than 528.8 eV for the bulk component. Therefore, the surface layer is well above  $2\lambda$  thick, i.e. ca. 30–50 Å. However, decomposition of the bulk phase cannot be concluded, since no differences could be observed with X-ray diffraction analysis. This has also been found in a number of other cases.<sup>10,11</sup> The surface layer

transformations are also manifested in the quantitative analysis presented in Table 2. Clearly, after use, large variations in the Y–Ba–Cu concentrations are obtained in conformity with a heterogeneous surface composed of several phases. Note that very high surface copper concentrations may be obtained after use at low oxygen pressures, which are associated with decreased Y/Ba ratios.

#### O 1s and Cu 2p Spectra

The various surface compositions obtained as a function of oxygen pressure during the oxidation of toluene affect mainly the oxygen and copper lines. In the O 1s spectra, see Fig. 9, an increased intensity on the low  $E_b$  side of the main peak is particularly intense for spectrum D. This used sample has the highest surface copper concentration, therefore we may connect this oxygen species with the surface copper com-

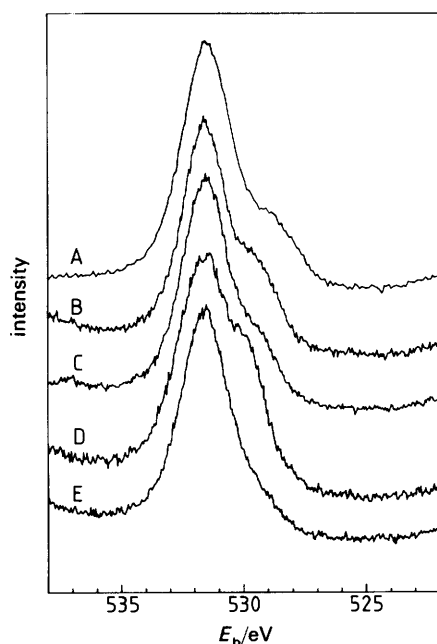


**Fig. 9** O 1s spectra for YBa<sub>2</sub>Cu<sub>3</sub>O<sub>7</sub> (A–D) and YBa<sub>2</sub>Cu<sub>3</sub>O<sub>6</sub> (E) catalysts before and after use at different oxygen partial pressures. A, Fresh catalyst; B, used at 200 Torr of oxygen; C, used at 48 Torr of oxygen; D, used at 10 Torr of oxygen; E, used at 4–8 Torr of oxygen

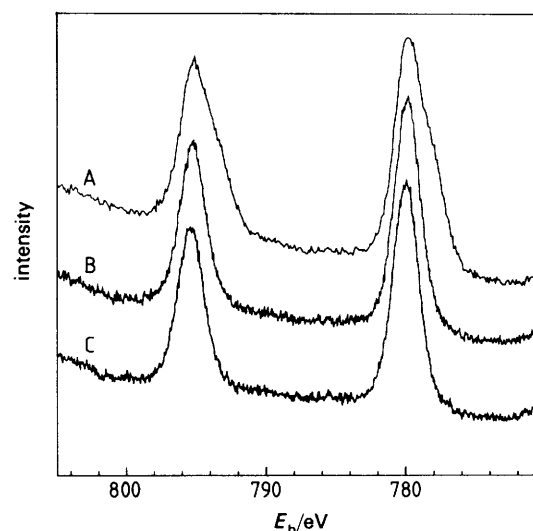


**Fig. 10** Ba 3d spectra for YBa<sub>2</sub>Cu<sub>3</sub>O<sub>7</sub> (A, B) and YBa<sub>2</sub>Cu<sub>3</sub>O<sub>6</sub> (C) catalysts before and after use at different oxygen partial pressures. A, Fresh catalyst; B, used at 200 Torr of oxygen; C, used at 4–8 Torr of oxygen

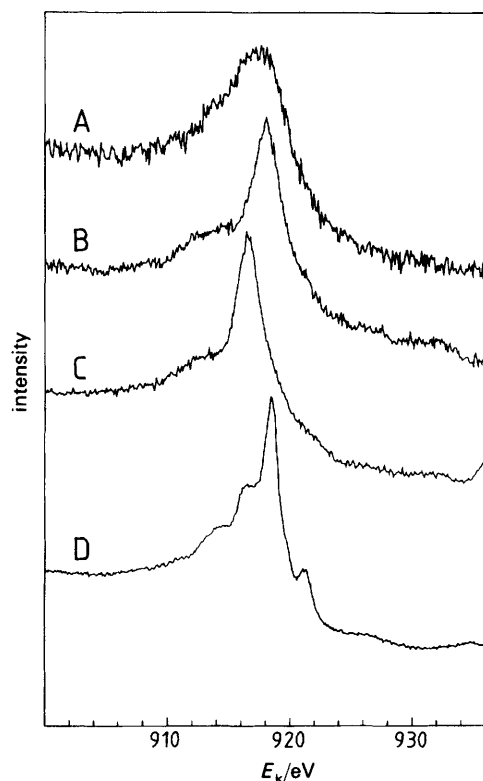


Fig. 11 Cu  $L_{3}M_{4.5}M_{4.5}$  spectra for  $YBa_{2}Cu_{3}O_{7}$  catalysts before and after use at different oxygen partial pressures. A, Fresh catalyst; B, used at 48 Torr of oxygen; C, used at 10 Torr of oxygen; D, Cu metal

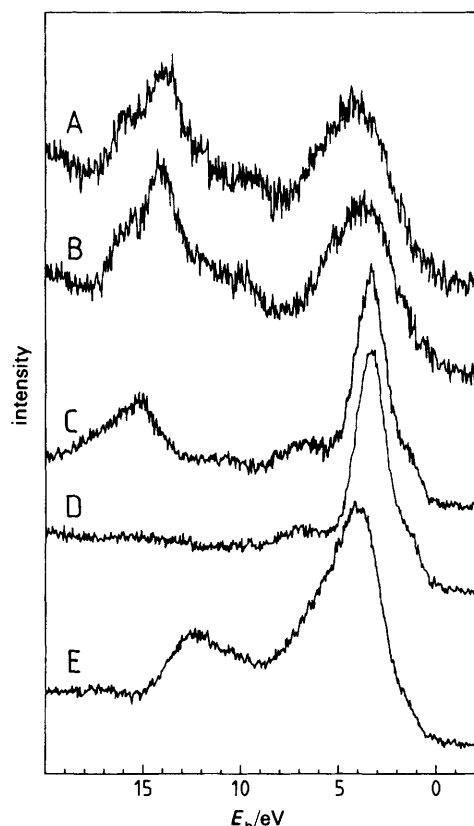


Fig. 12 Valence-band spectra for  $YBa_{2}Cu_{3}O_{7}$  catalysts before and after use at different oxygen partial pressures. A, Fresh catalyst; B, used at 200 Torr of oxygen; C, used at 10 Torr of oxygen; D,  $Cu_{2}O$ ; E,  $CuO$

Table 2 Content of metals in atom% calculated from XPS data for Y-Ba-Cu-O catalysts, as received and used at different reaction conditions

sample	Fig. <sup>a</sup>	$P_{O_2}$ /Torr	atom%		
			Y	Ba	Cu
$YBa_{2}Cu_{3}O_{7-x}$					
fresh	—	—	14	32	54
fresh, after air storage for 6 months	—	—	18	44	38
used	3, 4	200	28	39	33
used	7, 8	48	12	48	40
used	5, 6	10	6	24	69
$YBa_{2}Cu_{3}O_{6+x}$					
used	1, 2	4-8	21	44	35

<sup>a</sup> Catalysts used as given in the various figures prior to XPS analysis.

pounds. After use at high oxygen pressures, spectra B and C, this feature appears at an  $E_b$  slightly lower than that after use at low oxygen pressures, spectra D and E. This difference is in conformity with the lower O 1s  $E_b$  for  $CuO$  than for  $Cu_2O$ , see Table 1, as we may associate high oxygen pressures with  $Cu^{II}$  and low oxygen pressures with  $Cu^I$ , predominantly. This is corroborated by the Cu  $2p_{3/2}$  and  $L_{3}M_{4.5}M_{4.5}$  spectra, see Table 1 and Fig. 11. The  $Cu^{II}$  state is associated with the presence of a strong satellite structure<sup>23,24</sup> since two different final states are possible with different d electron counts. The ligand to 3d electron transfer, feasible for  $Cu^{II}$ , is not possible for  $Cu^I$  with a  $d^{10}$  configuration. Thus, the Cu 2p spectra clearly show the predominance of  $Cu^{II}$  at high oxygen pressure and complete absence of  $Cu^{II}$  at low oxygen pressure. The Cu 2p  $E_b$  shift between  $Cu_2O$  and Cu, see Table 1, is too small to allow identification of either one of these. However, the Cu  $L_{3}M_{4.5}M_{4.5}$  Auger spectra, shown in Fig. 11, allow identification of exclusively  $Cu^I$  in samples used at low oxygen pressure. This is also evident from the Auger parameter, see Table 1, which allows separation of  $Cu^0$ ,  $Cu^I$  and  $Cu^{II}$  independent of any possible errors in  $E_b$  measurements due to charging effects.

#### Valence-band Spectra

The valence-band spectra shown in Fig. 12 give further support for these conclusions. Three features are seen in the spectra. The structure between  $E_F$  and ca. 8 eV reflects the Cu—O derived states,  $Cu 3d^{10}$ ,  $O 2p^5$  and  $O 2p^6$ .<sup>25</sup> It is in these states that the main difference is seen upon use of the catalysts. The Ba 5p structure appears between 12 and 18 eV, with contributions from a Cu  $3d^8$  satellite at ca. 14 eV.<sup>26</sup> The intensity between ca. 8 and 13 eV seen for fresh catalysts and those used at high oxygen pressure is probably caused by certain Cu  $3d^9$  states associated with  $Cu^{II}$ , as for  $CuO$ .<sup>25</sup> The carbonate and hydroxylate contaminants present in the surface of these samples yield some photoemission intensity in this region.<sup>27</sup> Use of catalysts at high or low oxygen pressure gives very different VB spectra, B and C in Fig. 12, in conformity with the presence of either  $Cu^{II}$  or  $Cu^I$ . The narrow peak at 3.5 eV, spectrum C, due to the Cu  $3d^{10}$  state of  $Cu^I$  and a disappearance of the satellite structure of the  $Cu^{II}$  states, exemplifies particularly well the chemical differences.

## Discussion

### Surface Composition

The XPS results presented here show that the  $YBa_{2}Cu_{3}O_6$  and  $YBa_{2}Cu_{3}O_7$  catalysts are covered with a surface layer

containing degradation products. Its thickness is estimated to be well over 30–50 Å, but the bulk structure is retained as seen by XRD analysis. These results are in conformity with earlier results for ammoxidation catalysts.<sup>10,11</sup> The composition of the catalysts varies with the process conditions, mainly influenced by the oxygen pressure, giving exclusively Cu<sup>I</sup> states at low oxygen pressure and Cu<sup>II</sup> states at high oxygen pressure. The heterogeneous nature of the surface layer is reflected by its variable elemental composition. Note the frequent large increase in surface copper concentration caused by use at low oxygen pressures. Simultaneously, a large reduction of the Y/Ba ratio is obtained. Even a complete disappearance of Y core lines for samples used at extreme temperatures has been observed. From angular-dependent studies, the composition of the outermost surface layer of fresh YBa<sub>2</sub>Cu<sub>3</sub>O<sub>7-x</sub> was suggested to be Y<sub>0.01</sub>Ba<sub>1.02</sub>Cu<sub>1</sub>O<sub>2.2</sub>, or rather BaCuO<sub>2</sub><sup>21</sup> and accounted for by the easy diffusion of Ba and Cu towards the surface.<sup>28</sup> BaCuO<sub>2</sub> has also been suggested as a decomposition product of the green phase, Y<sub>2</sub>BaCuO<sub>5</sub>.<sup>22</sup> When BaCuO<sub>2</sub> is exposed to moisture and carbon dioxide at atmospheric pressure, it is likely that BaCO<sub>3</sub> crystallites nucleate and grow, leaving areas of copper oxide. The presence of highly dispersed surface copper oxides is suggested by the large similarity between the XP spectra of samples used at low or high oxygen pressures and those for Cu<sub>2</sub>O and CuO, respectively. It is further supported by atom-probe microscopy studies revealing extremely Cu-rich regions separated from extremely Ba-rich regions by distances of only 2.5–5.0 nm.<sup>29</sup>

### Catalytic Performance

The rate and selectivity of toluene oxidation over YBa<sub>2</sub>Cu<sub>3</sub>O<sub>7</sub> and YBa<sub>2</sub>Cu<sub>3</sub>O<sub>6</sub> are strongly dependent on the oxygen partial pressure. The rate is greatly increased between *ca.* 10 and 50 Torr oxygen, whereas the selectivity is greatly decreased at high oxygen pressures. This is typical behaviour for these materials, and is well documented for ammoxidation of toluene.<sup>8–11</sup> As found in this work on the oxidation of toluene, the low activity at low oxygen partial pressure is associated with the formation exclusively of Cu<sup>I</sup> surface states, at the probing depth of XPS. Likewise, the high activity at high oxygen partial pressure is due to formation exclusively of almost pure Cu<sup>II</sup> surface states. However, the bulk structure, *i.e.* the oxygen stoichiometry or *x* value, also appears to show a definite influence on the activity.<sup>2,9–11</sup> The simple fact that at low oxygen partial pressures only Cu<sup>I</sup> states are observed also shows that the original bulk structure is not retained at the surface. The hysteresis effects observed, when increasing and decreasing the oxygen partial pressure, may indicate that considerable structural rearrangements, with dispersion and segregation, occur within this decomposed surface layer with the different treatments. This is supported by the large changes in the Cu 2p<sub>3/2</sub> peak intensities, which were also observed earlier.<sup>10</sup>

In earlier work on ammoxidation of toluene<sup>10,11</sup> the catalyst was modelled as consisting of highly dispersed copper oxides, strongly influenced by the oxygen content of the bulk material. In this work on toluene oxidation, it is additionally shown that the initial state of the fresh catalyst is less important than the pretreatment procedures. The initial pretreatment has normally been to heat YBa<sub>2</sub>Cu<sub>3</sub>O<sub>6</sub> samples in nitrogen and YBa<sub>2</sub>Cu<sub>3</sub>O<sub>7</sub> samples in oxygen to bring their compositions closer to the nominal composition. The catalytic measurements are therefore logically performed over YBa<sub>2</sub>Cu<sub>3</sub>O<sub>6</sub> at low oxygen pressures, and over YBa<sub>2</sub>Cu<sub>3</sub>O<sub>7</sub> at high oxygen pressures initially, followed by increased or decreased oxygen pressures, respectively. Moreover, when

comparing their catalytic performances it would appear, as seen in Fig. 1–4, that catalysts of initial composition YBa<sub>2</sub>Cu<sub>3</sub>O<sub>6</sub> are superior. However, this is not a permanent condition as seen by the continued activity measurements, see Fig. 1–4, showing hysteresis effects and data for YBa<sub>2</sub>Cu<sub>3</sub>O<sub>7</sub> similar to those initially obtained for YBa<sub>2</sub>Cu<sub>3</sub>O<sub>6</sub>. This impression is further strengthened by Fig. 5 and 6, showing that an even higher selectivity than measured initially for YBa<sub>2</sub>Cu<sub>3</sub>O<sub>6</sub> is obtained for an extensively used YBa<sub>2</sub>Cu<sub>3</sub>O<sub>7</sub> after heat treatment in nitrogen. A reductive treatment even increases its performance. However, complete reduction or oxidation leads to an inferior catalyst. The data suggest that a largely reduced YBa<sub>2</sub>Cu<sub>3</sub>O<sub>7</sub> or slightly oxidized YBa<sub>2</sub>Cu<sub>3</sub>O<sub>6</sub> catalyst gives optimum performance.

The rate of the disappearance of toluene, observed at low oxygen partial pressure, is *ca.* 500 μmol g<sup>-1</sup> h<sup>-1</sup>, which is similar to the rates observed in ammoxidation of toluene at low oxygen pressures.<sup>10,11</sup> The selectivity is, however, not at all comparable. The highest stable selectivity for benzaldehyde, presented here, is *ca.* 12%, although it should be realized that the selectivity, as well as the activity, appears to be rather dependent on the pretreatment of the sample. This material thus fails to be highly selective in the oxidation of toluene, though it shows a very high selectivity for benzonitrile in the ammoxidation of toluene under proper conditions.

Since the rate of toluene disappearance is of the same order of magnitude for both oxidation and ammoxidation, it seems reasonable to assume that the same initial intermediate is present in both reactions. This intermediate is probably formed in the first hydrogen abstraction process. The different selectivities are then explained by the different possible further reactions of the initial intermediate in both cases. In ammoxidation, the surface will be saturated by adsorbed ammonia species, possibly imido species, and there will then be a high overall rate of reaction between both intermediates leading finally to formation of benzonitrile. Also important may be that benzonitrile is a considerably more stable product than benzaldehyde. In oxidation, on the other hand, the most abundant species available for continued reaction of the intermediate are various oxygen species, which on these surfaces are very likely to be electrophilic, and thus lead mainly to combustion.

### Catalyst Model

From the discussion above it appears that it would be difficult to neglect the possible importance of highly dispersed surface copper oxides on the catalytic properties. This is corroborated by literature data reporting similar selectivity effects for copper oxide catalysts in the oxidation of propene, with selective oxidation at low oxygen pressures and unselective oxidation at high pressures.<sup>30–32</sup> Earlier, interpretations in terms of site isolation<sup>30</sup> and band theory<sup>31</sup> were attempted, but the various crystal structures of the copper oxides were not taken into consideration. This is done in the present work by comparing coordinations and formal charges obtained by bond-valence calculations.

As a model of the catalyst for total combustion we consider the ideal surfaces of fully oxidized CuO, since Cu<sup>II</sup> states are prevailing under these conditions as seen by XPS. These surface structures may, in the first approximation, be assumed as those obtained by cutting a crystal in various directions with the structure retained. None of these ideal surfaces are saturated, as seen from the structure in Fig. 13 and bond valences given in Table 3. It is conceivable that coordinatively unsaturated Cu and O species are formed, corresponding to free bond valences of close to 0.5 for Cu and 1 for O. Thus, formally one could speak of Cu<sup>+1.5</sup> and O<sup>-</sup>

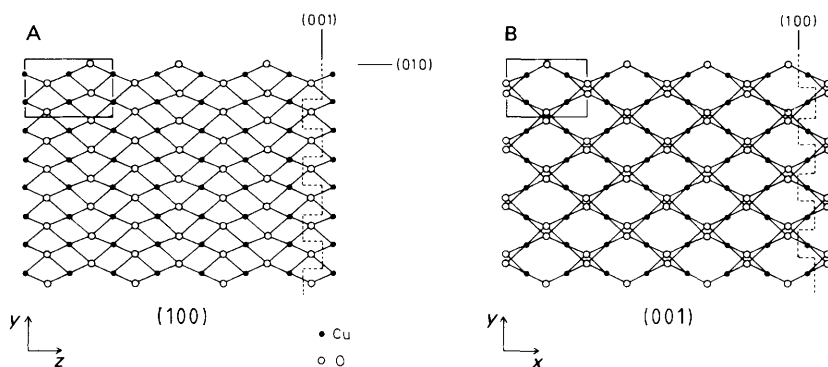


Fig. 13 Structure of CuO. Viewed along: A, *a* axis; B, *c* axis. (Thin lines mark unit cell and dashed lines considered cleavage planes)

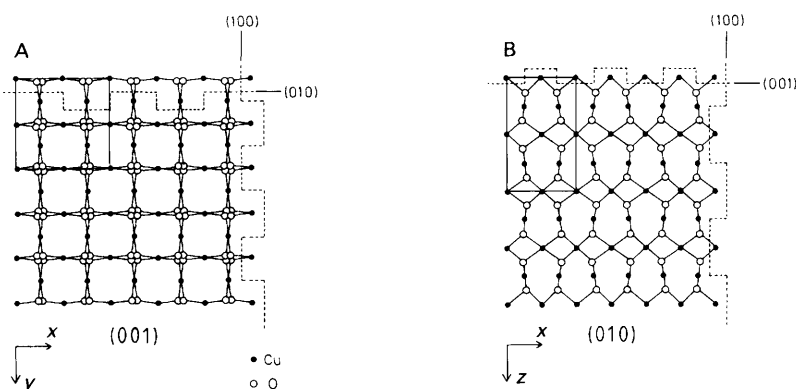


Fig. 14 Structure of  $\text{Cu}_{16}\text{O}_{14}$ . Viewed along: A, *c* axis; B, *b* axis. Comments as in Fig. 13

surface species. These Cu species are adjacent, two by two, and easy formation of  $\text{O}_2^-$  species seems plausible. It is understandable that such a surface is highly reactive towards total combustion, which would be favoured by a high concentration of these various species. A complete coverage with O species is considered undesirable.

The effect of a partial reduction of CuO is exemplified by bond-valence calculations for the mineral paramelaconite with the formula  $\text{Cu}_{16}\text{O}_{14}$ ,<sup>36</sup> see Fig. 14 and Table 3. At the various low-Miller-index surface planes, a free bond valence of *ca.* 1 for Cu and 0.36–0.7 for O, corresponding formally to

$\text{Cu}^{+1}$  and  $\text{O}^{-1.3}$ – $\text{O}^{-1.7}$ , may be expected. These O species are less electrophilic than for CuO, but over  $\text{Cu}^{+1}$ , adsorbed  $\text{O}_2^-$  and  $\text{O}^-$  could be formed in competition with hydrocarbon adsorption.

The catalyst for selective oxidation is modelled as  $\text{Cu}_2\text{O}$ , since, as seen by XPS, only  $\text{Cu}^{\text{I}}$  states are present. A consideration of the structure and bond valences, see Fig. 15 and Table 3, suggests that on the primitive surfaces of  $\text{Cu}_2\text{O}$ , Cu and O species with free bond valences of *ca.* 0.5 are formed. These correspond formally to  $\text{Cu}^{+0.5}$  and  $\text{O}^{-1.5}$ . The selective properties of  $\text{Cu}_2\text{O}$  can then be interpreted in terms of

Table 3 Bond lengths, bond valences and bond valence sums for copper oxides

oxide	bond	bond distance/Å	bond valence	
			$\text{Cu}^{2+}$ <sup>a</sup>	$\text{Cu}^{2+}$ <sup>b</sup>
$\text{CuO}^c$	Cu—O	$1.9509 \times 2$	$0.4560 \times 2$	$0.4559 \times 2$
	Cu—O	$1.9608 \times 2$	$0.4439 \times 2$	$0.4450 \times 2$
	Cu—O	$2.7840 \times 2$	$0.072 \times 2$	$0.072 \times 2$
			$\sum 1.93$	$\sum 1.94$
$\text{Cu}_{16}\text{O}_{14}^d$	Cu—O	$1.801 \times 2$	$0.702 \times 2$	$0.727 \times 2$
	Cu—O	$2.035 \times 2$	$0.363 \times 2$	$0.377 \times 2$
			$\sum 2.13$	$\sum 2.20$
			$\text{Cu}^{2+}$	$\text{Cu}^{1+}$
$\text{Cu}_2\text{O}^e$	Cu—O	$1.84 \times 2$	$0.626 \times 2$	$0.525 \times 2$
			$\sum 1.25$	$\sum 1.05$

<sup>a</sup> Ref. 33,  $S = S_0(R/R_0)^{-N}$ , constants from ref. 34. <sup>b</sup> Ref. 34,  $S = Z(0.1177 - 0.0081Z - 0.0347r_0 - 0.0050Zr_0)/(R - R_0)$ , constants from ref. 35. <sup>c</sup> Ref. 33. <sup>d</sup> Ref. 36. <sup>e</sup> Ref. 37.

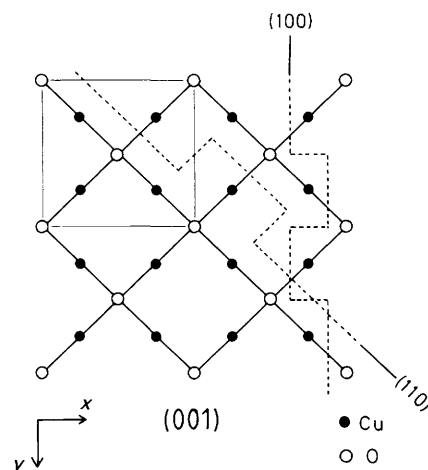


Fig. 15 Structure of  $\text{Cu}_2\text{O}$ . Viewed along *c* axis. Comments as in Fig. 13

the less electrophilic  $O^{-1.5}$  species and by the lower oxidizing power of the  $Cu^{+0.5}$  species. It is thus concluded that the availability of electrophilic oxygen species and the redox properties of the Cu cation are decisive for the catalytic properties.

The National Energy Administration is acknowledged for financial support.

## References

- N. Mizuno, M. Yamato and M. Misono, *J. Chem. Soc., Chem. Commun.*, 1988, 887.
- A. Jiang, Y. Peng, Q. Zhou, P. Gao, H. Yan and J. Deng, *Catal. Lett.*, 1989, **3**, 235.
- J. C. Otamiri and S. L. T. Andersson, *Appl. Catal.*, 1991, **73**, 267.
- J. G. McCarty, M. A. Quinlan and H. Wise, in *Proc. 9th Int. Congr. Catal.*, Ottawa, Canada, 1988, The Chemical Institute of Canada, 1988, vol. 4, p. 1818.
- I. Lee and K. Y. S. Ng, *Catal. Lett.*, 1989, **2**, 403.
- D. Klissurski, J. Pesheva, Y. Dimitriev, N. Abadjieva and L. Minchev, in *New Developments in Selective Oxidation*, *Stud. Surf. Sci. Catal.*, ed. G. Centi and F. Trifiro, Elsevier, Amsterdam, 1990, vol. 55.
- I. Hálasz, *Appl. Catal.*, 1989, **47**, L17.
- S. Hansen, J. C. Otamiri, J.-O. Bovin and A. Andersson, *Nature (London)*, 1988, **344**, 143.
- J. C. Otamiri, A. Andersson, S. Hansen and J.-O. Bovin, in ref. 6, p. 275.
- J. C. Otamiri, S. L. T. Andersson and A. Andersson, *Appl. Catal.*, 1990, **65**, 159.
- J. C. Otamiri, A. Andersson, S. L. T. Andersson, J. E. Crow and Y. Gao, *J. Chem. Soc., Faraday Trans.*, 1991, **87**, 1265.
- S. Hansen, J. C. Otamiri and A. Andersson, *Catal. Lett.*, 1990, **6**, 33.
- S. L. T. Andersson and J. C. Otamiri, *Appl. Surf. Sci.*, 1990, **45**, 1.
- M. M. Garland, *J. Mater. Res.*, 1988, **3**, 830.
- S. L. T. Andersson, *J. Chromatogr. Sci.*, 1985, **23**, 17.
- M. F. Yan, R. L. Barns, H. M. O'Bryan Jr., P. K. Gallagher, R. C. Sherwood and S. Jin, *Appl. Phys. Lett.*, 1987, **51**, 532.
- I. Nakada, S. Sato, Y. Oda and T. Kohara, *Jpn. J. Appl. Phys.*, 1987, **26**, L697.
- J. H. Thomas III and M. E. Labib, in *Thin Film Processing and Characterization of High-temperature Superconductors*, Anaheim, CA, 1987, ed. J. M. E. Harper, R. J. Colton and L. C. Feldman, AIP Conf. Proc. No. 165, American Vacuum Society Series 3, American Institute of Physics, New York, 1988, p. 374.
- R. G. Egdell, W. R. Flawell and P. C. Hollamby, *J. Solid State Chem.*, 1989, **79**, 238.
- B. G. Hyde, J. G. Thompson, R. L. Withers, J. G. Fitzgerald, A. M. Stewart, D. J. M. Bevan, J. S. Anderson, J. Bitmead and M. S. Paterson, *Nature (London)*, 1987, **327**, 402.
- C. C. Chang, M. S. Hedge, X. D. Wu, B. Dutta, A. Inam, T. Venkatesan, B. J. Wilkens and J. B. Wachtman Jr., *J. Appl. Phys.*, 1990, **67**, 7483.
- V. I. Nefedov, A. N. Sokolov, M. A. Tyzykhov, N. N. Oleinikov, Ye. A. Yeremina and M. A. Kolotyrkina, *J. Electron Spectrosc. Relat. Phenom.*, 1989, **49**, 47.
- G. Schön, *Surf. Sci.*, 1973, **35**, 96.
- G. van der Laan, C. Westra, C. Haas and G. A. Sawatzky, *Phys. Rev. B*, 1981, **23**, 4369.
- F. Parmigiani and G. Samoggia, *Europhys. Lett.*, 1988, **7**, 543.
- J. H. Weaver, H. M. Meyer III, T. J. Wagener, D. M. Hill, Y. Gao, D. Peterson, Z. Fisk and A. J. Arko, *Phys. Rev. B*, 1988, **38**, 4668.
- S. L. Qui, M. W. Ruckman, N. Brookes, P. D. Johnson, J. Chen, C. L. Lin, M. Strongin, B. Sinkovic, J. E. Crow and C.-S. Jee, *Phys. Rev. B*, 1988, **37**, 3747.
- T. Venkatesan, C. C. Chang, D. Dijkamp, S. B. Ogale, E. W. Chase, L. A. Farrow, D. M. Hwang, P. F. Miceli, S. A. Schwarz, J. M. Tarascon, X. D. Wu and A. Inam, *J. Appl. Phys.*, 1988, **63**, 4591.
- O. Nishikawa and M. Nagai, *Phys. Rev. B*, 1988, **37**, 3686.
- J. L. Callahan and R. K. Grasselli, *AIChE J.*, 1963, **9**, 755.
- B. J. Wood, H. Wise and R. S. Yolles, *J. Catal.*, 1969, **15**, 355.
- A. Amariglio, O. Benali and H. Amariglio, *J. Catal.*, 1989, **118**, 164.
- S. Åsbrink and L.-J. Norrby, *Acta Crystallogr., Sect. B*, 1970, **26**, 8.
- I. D. Brown and R. D. Shannon, *Acta Crystallogr., Sect. A*, 1973, **29**, 266.
- J. Ziolkowski, *J. Solid State Chem.*, 1985, **57**, 169.
- N. Datta and J. W. Jeffery, *Acta Crystallogr., Sect. B*, 1978, **34**, 22.
- P. Niggli, *Z. Kristallogr.*, 1922, **57**, 253.

Paper 1/045221; Received 29th August, 1991